

Reviewed Preprint

v1 • June 30, 2026

Not revised

✉ For correspondence:

bw5h@virginia.edu

cd2fj@virginia.edu

Competing interests: No

competing interests declared

Funding: See page 18

Reviewing editor: Anne E West,
Duke University, United States© 2026, Sewell et al. This article is
distributed under the terms of the[Creative Commons Attribution](#)[License](#), which permits unrestricted
use and redistribution provided that
the original author and source are
credited.

A Single-Cell Signaling Atlas of Spinal Cord BDNF Responses Reveals Determinants Beyond Receptor Expression

Jonathon M Sewell^{1,2,4}, Autumn C Bissett², Grace Lee³, Eli R Zunder³, Bettina Winckler¹✉,
Chris D Deppmann^{1,2,3}✉¹Department of Cell Biology, School of Medicine, University of Virginia, Charlottesville, United States • ²Department of Biology, College of Arts and Sciences, University of Virginia, Charlottesville, United States • ³Department of Biomedical Engineering, School of Medicine, University of Virginia, Charlottesville, United States • ⁴Cell and Developmental Biology Graduate Program, School of Medicine, University of Virginia, Charlottesville, United States

eLife Assessment

This study of BDNF signaling in heterogeneous spinal cord cultures provides a **fundamental** conceptual advance by demonstrating that cell identity and maturation state, rather than receptor stoichiometry alone, ultimately determine how a trophic message is interpreted, in a framework the authors call "prepared competence." The evidence is **compelling**, with the discrete subpopulation behavior, the maturation-dependent acquisition of signaling competence, and the dissociation between receptor abundance and signaling output emerging clearly from the high-dimensional dataset. This study will be of interest to neurobiologists as well as cell biologists who study the molecular basis of cell signaling.

<https://doi.org/10.7554/eLife.111513.1.sa3>

Abstract

Although the influence of Brain-Derived Neurotrophic Factor (BDNF) has been characterized across numerous neural settings, how individual cells decode this pleiotropic message into context-dependent signaling responses remains unresolved. Using highly multiplexed single-cell mass cytometry to simultaneously measure levels of 19 signaling markers and 18 cell ID markers, we constructed a temporal atlas of BDNF-induced signaling relative to two control conditions across diverse spinal cord lineages and maturation states. We demonstrate that not all cells contribute to the global BDNF response with ~47-75% of cells having increased ERK phosphorylation at peak activation. Our analysis of 20 uniquely identified cell identities reveals that TrkB/p75NTR receptor stoichiometry sets the potential for response, but ultimately the sustained reduction of surface TrkB predicts BDNF sensitivity. Surprisingly, identical receptor profiles in distinct cell types yield fundamentally different signaling responses, indicating that cell identity acts as the final arbiter of the BDNF message. These findings reframe BDNF sensitivity as a form of prepared competence. This work thus provides a framework for understanding how intracellular context dictates the functional interpretation of neurotrophic cues.

Introduction

Although Brain-Derived Neurotrophic Factor (BDNF) is a single molecular message, a mature homodimeric ligand (1), orchestrates many different neurobiological processes, from neurodevelopmental patterning to synaptic plasticity underlying learning and memory (2, 3). While the canonical model suggests that the receptor expression profile dictates the response (4,

5), the broad range of functional outcomes across the nervous system that are attributed to a single ligand implies that the ligand-receptor interaction alone is insufficient to explain the broad functional interpretations of the BDNF message.

The interplay between the receptors TrkB and p75NTR is widely viewed as a regulatory switch that tunes the BDNF signaling response. Upon ligand binding, TrkB autophosphorylates to initiate core Ras/MAPK, PI3K/Akt, and PLC-gamma cascades (6), yet these pathways are qualitatively and quantitatively modified by p75NTR co-expression. This interaction can synergistically enhance TrkB affinity (7–10), prolong signaling duration by reducing receptor ubiquitination (11), or independently activate NF-kappa-B and JNK/c-Jun stress-response pathways (2). However, because these mechanistic 'rules' were largely defined in transfected cell lines or restricted primary lineages, it remains unclear whether receptor stoichiometry alone can predict signaling outcomes across the heterogeneous cell populations of the nervous system. While single-cell signaling heterogeneity is a recognized feature of other receptor tyrosine kinase (RTK) systems (12), a systematic mapping of how cell identity and maturation state filter the BDNF message is currently unexplored.

This knowledge gap is primarily due to the reliance on biochemical techniques, such as immunoblotting, which measure an aggregate output that is blind to cellular heterogeneity. While these bulk readouts have provided a thorough profile of the BDNF signaling cascade, they cannot uncover how a single ligand might be differentially interpreted across non-uniform subpopulations (13). Newer single-cell technologies offer higher resolution but present contrasting trade-offs: single-cell RNA sequencing effectively maps cell identity but fails to capture the rapid, post-translational phosphorylation events that define the immediate BDNF response (4). Similarly, while standard fluorescence-based flow cytometry provides single-cell signaling data, it is constrained by spectral overlap, preventing the simultaneous measurement of the broad repertoire of phosphoproteins and receptor profiles required to decode a complex signaling landscape (14).

To resolve this decoding problem, we employed highly multiplexed single-cell mass cytometry to construct a high-resolution time course of BDNF signaling across neural lineages and maturation states. By simultaneously measuring receptor composition, receptor surface abundance, and a broad panel of downstream phosphoproteins, our data show a highly filtered signaling landscape where responsiveness is an emergent property of cell identity rather than a simple function of receptor abundance. Our results demonstrate that BDNF signaling is governed by a multi-layered gating system: (1) receptor levels initialize the potential for pathway induction, (2) a sustained reduction of surface TrkB serves as predictor of increased phosphorylation of downstream signaling effectors, and (3) cell-intrinsic environments act as the final arbiter of BDNF sensitivity. By moving beyond the 'average' signal of bulk biochemistry, we show that even identical receptor profiles yield distinct signaling profiles across cell types, reframing BDNF sensitivity as a form of prepared competence. This multi-layered regulation provides a framework for understanding how cellular context dictates the interpretation of the neurotrophic message.

Results

Single-cell mapping resolves a continuous maturation gradient and lineage diversity

To determine how individual neural identities respond to a uniform BDNF stimulus, we utilized single-cell mass cytometry to simultaneously quantify 19 signaling effectors across primary spinal cord cultures (E14 rat) (Fig. 1A, table S1-2). We selected E14 rat spinal cord as our model system because it provides a developmental window in which neural progenitors, neurons of varying maturity, and non-neuronal populations coexist within a single preparation. Thus, the heterogeneity of this culture system enabled our simultaneous assessment of BDNF signaling across multiple lineages and maturation states.

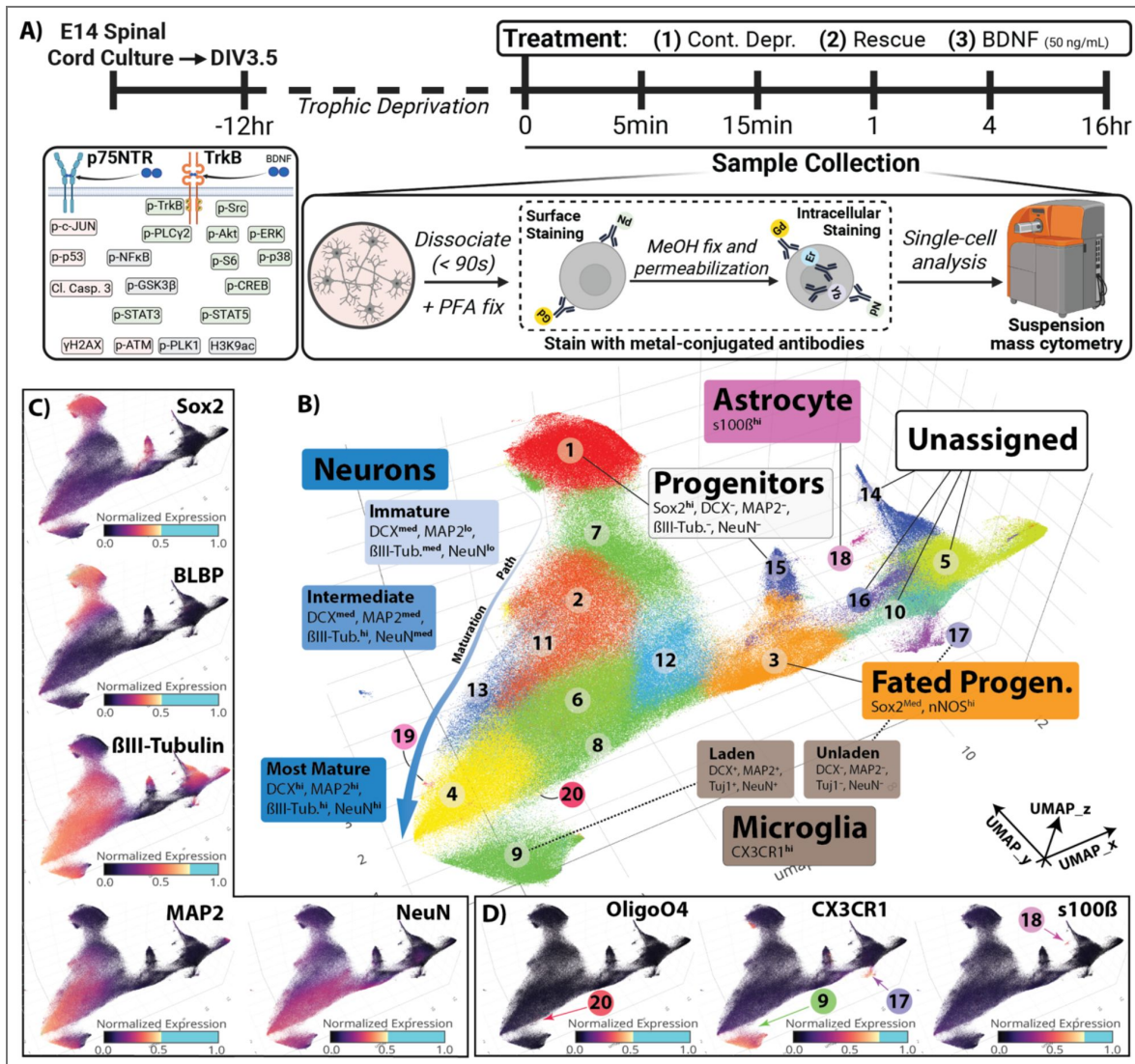


Fig. 1. Single cell mass cytometry identifies distinct cell types in rat embryonic spinal cord cultures.

(A) Embryonic day 14 (E14) rat spinal cord are cultured to day in vitro (DIV) 3.5 before a 12hr supplement starvation and subsequent treatment. Samples are collected at indicated time points by rapid dissociation (<90s) and fixation by 2% paraformaldehyde (PFA), then stored at -80°C. Samples are barcoded, pooled, and simultaneously stained with isotopically pure metal-conjugated antibodies before and after methanol (MeOH) permeabilization and fixation. Stained samples are then analyzed by single-cell (suspension) mass cytometry. Created using *BioRender*. (B) Leiden clustering by cell identity markers is visualized by dimensionality reduction on a 3-Dimensional Uniform Manifold Association Plot (UMAP) colored and labeled by identified cell types. (C) The resulting UMAP is colored by the level of individual cell identity markers to highlight the observed neuronal maturation gradient that shifts from Sox2+, BLBP+ progenitors to more mature neuronal identity with increasing levels of βIII-Tubulin, MAP2, and NeuN. (D) Non-neuronal cell identity marker levels are plotted to define glial cell populations. Individual cell identity marker expression is normalized from 0 to 1, and gradient is shifted to emphasize locations of marker enrichment, with cells above the intensity threshold colored cyan.

Leiden clustering of identity marker expression distinguished 20 unique cell populations (Fig. 1B [↗](#), fig. S1A [↗](#)), which were partitioned into four primary categories based on marker expression level (fig. S1A, B [↗](#)): Progenitor (Sox2+, 12.8%), Neuronal (β III-tubulin+, 52.5%), Non-Neuronal (17.0%), and Unassigned (17.6%). Unassigned cells represent those that could not be unambiguously defined by our panel of identity markers.

Notably, based on expression levels of neuronal identity markers, we were able to resolve a developmental trajectory originating from Sox2+ progenitors (Cluster 1), through intermediate immature neurons (Clusters 7, 2, 13), to the most mature NeuN-hi neurons (Cluster 4) (Fig. 1C [↗](#), Fig. S1D [↗](#)). We identified additional Non-Neuronal cell types, including nNOS+ fated progenitors, astrocytes (s100 β +), oligodendrocytes (OligoO4+) and microglia (CX3CR1+) based on their distinguishing identity marker (Fig. 1C [↗](#), Fig. S1A, B [↗](#)). Microglia can be further classified based on the presence (“laden”) or absence (“unladen”) of neuronal identity markers, which may represent the phagocytic state of these CX3CR1+ cells. By resolving this maturation gradient and the cell-type heterogeneity at single-cell resolution, we established a high-dimensional system to test to what extent BDNF signaling is a universal event or a state-dependent property of specific lineages.

The global BDNF response is driven by a discrete subpopulations of cells

To determine if our platform recapitulated well-established canonical signaling profiles, we first aggregated our single-cell data into a “pseudobulk” format to assess the global response to BDNF (fig. S2-3 [↗](#)). As expected, BDNF induced rapid activation across core Ras/MAPK and PI3K/Akt pathways, including pERK, pAkt, and pCREB, relative to controls where BDNF deprivation was continued (Fig. 2A [↗](#), fig. S4A [↗](#)). These responses were largely abrogated by the Trk inhibitor K252a (Fig. 2B [↗](#), fig. S4A [↗](#)). In addition, BDNF stimulation exhibited a unique phosphoproteomic response which was distinct from the general trophic rescue elicited by refeeding with rich medium (“Rescue”) (fig. S5 [↗](#)), confirming the specificity of the BDNF stimulus.

However, single-cell analysis indicates that these aggregate trends obscure highly heterogeneous responses. Even at peak activation (15 min), the population did not respond uniformly, but instead discrete subpopulations, ranging from 47% to 75% of cells, responded (Fig. 2C [↗](#), fig. S4B [↗](#), table S3 [↗](#)). This observation provides evidence that BDNF responsiveness is not a uniform population event but is restricted to specific cellular contexts (Fig. 2D [↗](#)).

Maturation state and cell identity regulate BDNF signaling competency

We next determined if the heterogeneity of BDNF responsiveness was structured by cell identity, for instance if neuronal cells responded and non-neuronal cells did not. While both neuronal and non-neuronal cells show increased activation of established pathways (fig. S6A [↗](#)), neuronal cells exhibit a greater magnitude of change (fig. S6B [↗](#)). Inhibition of Trk activity with K252a significantly reduces BDNF-induced activation to control or near-control levels in both cell type categories (fig. S6C [↗](#)).

A more granular assessment of cell-type-specific pathway activation revealed a diversity of responsiveness (Fig. 3A-B [↗](#), fig. S7A [↗](#)). Intriguingly, we observed a maturation-dependent acquisition of signaling competence along the neuronal lineage. Sox2+ progenitors remained relatively signaling-silent (1.7-fold pERK) compared to intermediate and mature neurons, which exhibited a 16.2- to 17.2-fold induction at the same time point (Fig. 3C [↗](#), table S4 [↗](#)).

Crucially, progenitors showed robust activation when treated with rescue media (Fig. 3D [↗](#), table S4 [↗](#)), confirming that they are intrinsically signaling-competent but specifically insensitive to BDNF. Further comparison of treatment-dependent responses shows a relatively consistent response to rescue media along the neuronal lineage, suggesting that maturation-dependent responsiveness is not generalizable to any stimulation (fig. S8 [↗](#)).

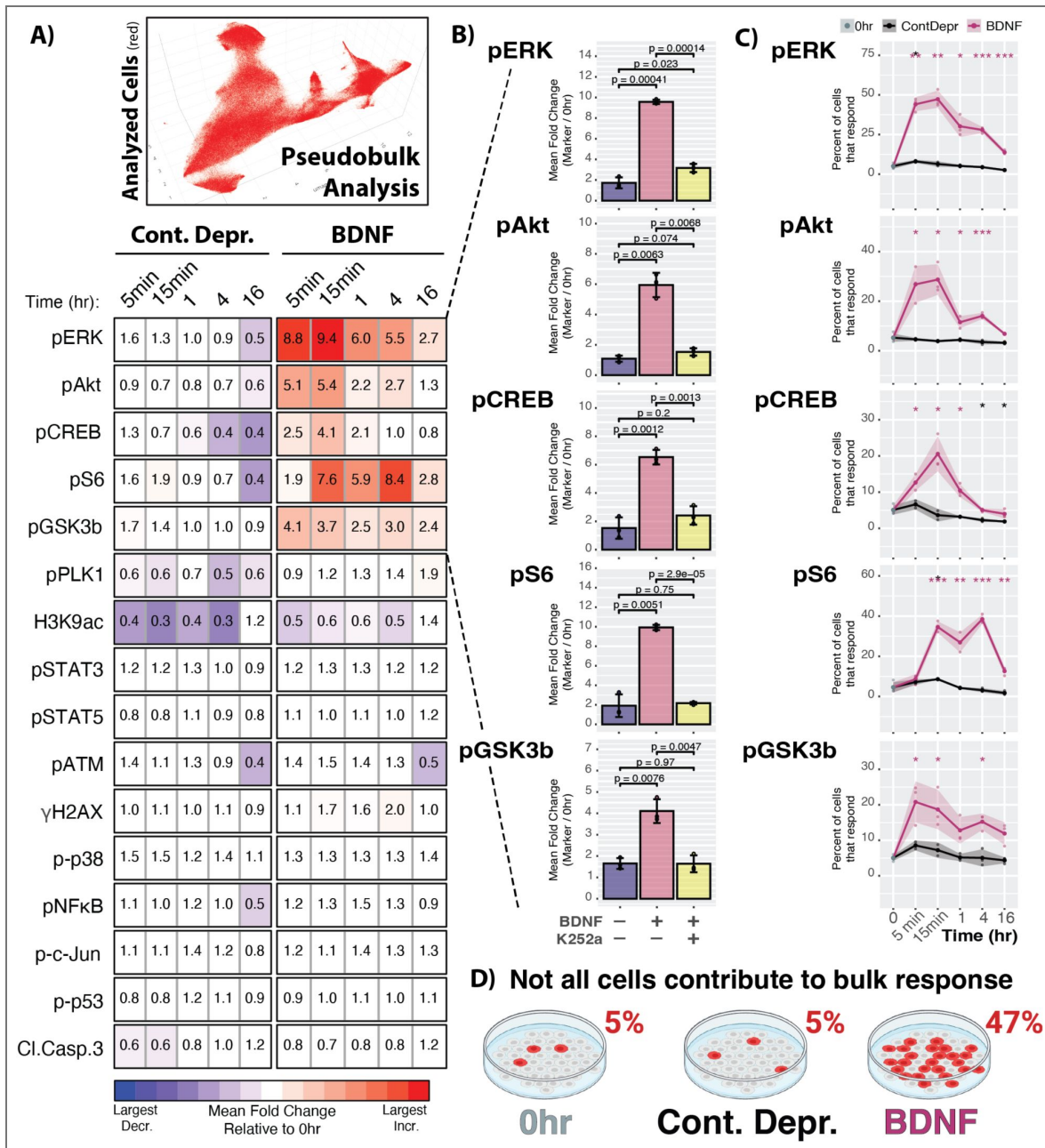


Fig. 2. Pseudobulk analysis defines responsive subpopulation of cells responsible for global BDNF-induced signaling.

(A) All cells were included in the pseudobulk analysis of the mean fold change (FC) of responsive cells relative to 0hr, as depicted by heatmap for select markers across time after either continued deprivation (Cont. Depr.) or BDNF treatment. No change is indicated by white ($0.67 < FC < 1.5$), the level of decrease is visualized by a blue scale ($FC \leq 0.67$), and the level of increase is visualized by a red scale ($FC \geq 1.5$). Values represent the mean FC (0hr, $n = 4$; Cont. Depr., $n = 2-3$; BDNF, $n = 3$). (B) Co-treatment of BDNF with a Trk inhibitor (K252A) largely abrogated BDNF-induced responses at 1hr of treatment ($n = 3$). (C) The percent of cells that are defined as responsive plotted for individual signaling markers across time (0hr, $n = 4$; Cont. Depr., $n = 2-3$; BDNF, $n = 3$). (D) Schematic visualization depicting the cells that contribute to a bulk readout, where not all treated cells respond to the stimulus. Created in *BioRender*. (B, C) Individual points indicate replicate values summarized by mean \pm SD; p-values are relative to the 0hr samples, colored by treatment, and determined by unpaired Student t test (* $p < 0.05$; ** $p < 0.01$; *** $p < 0.001$ - see Supplemental Table 3 for values).

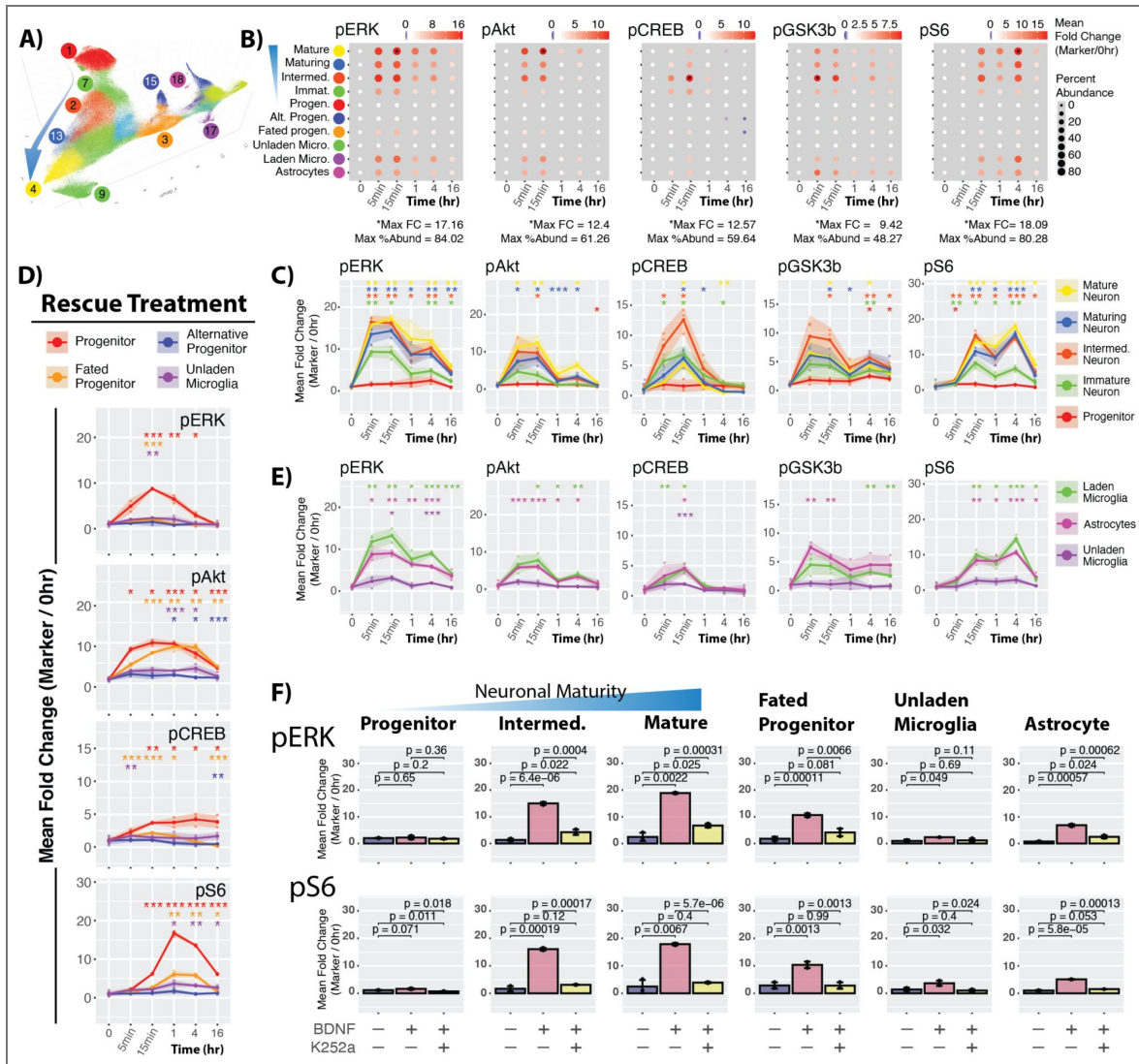


Fig. 3. BDNF-induced signaling dynamics differ between identified cell types.

(A) UMAP highlighting cell identity clusters that are subsequently analyzed. (B) Dot plot depicting the percent of cells that increase activation of the selected signaling molecule within each identified cell type. Size indicates the percent of the given cell type that contribute to the response, while color indicates the mean fold change relative to 0hr. (C) Line graph representation of select data from (B) emphasizes the comparison of responsive cells in the neuronal maturation path. (D) Signaling responses to rescue treatment in cell types that do not exhibit a robust response to BDNF. (E) Line graph representation of select data from (B) to compare responses in non-neuronal cell types. (F) Co-treatment of BDNF with a Trk inhibitor (K252A) largely abrogated cell-type-specific BDNF-induced responses at 1hr of treatment (n = 3). (C-F) Individual points indicate replicate values (0hr, n = 4; Rescue, n = 2-3; BDNF, n = 3) and summarized by mean±SD. p-values are relative to the 0hr samples, colored by cell type, and determined by unpaired Student t test (* p < 0.05; ** p < 0.01; *** p < 0.001 - see Supplemental Table 4 for values). All FC values calculated as described in Supplemental Figure 2 for each cell type.

Non-neuronal lineages similarly showed divergent sensitivity: astrocytes and “laden” microglia were highly responsive, whereas “unladen” microglia remained signaling-silent (Fig. 3E). Furthermore, while the Trk-inhibitor K252a blunted most activated pathways, the failure to completely abolish pERK induction in several lineages (Fig. 3F, fig. S7B, table S4) suggests that Trk activity is not the sole determinant of the signaling patterns, hinting at additional cell-intrinsic regulatory layers.

Unsupervised clustering reveals cell identity-dependent BDNF signaling signatures

By measuring 19 signaling markers at once, we were able to define signaling patterns in identified cell types based on the temporal changes of individual marker abundance. However, assessing each marker separately limits our analysis and does not take advantage of our multi-dimensional dataset. Thus, before exploring the observation of Trk-activity dependence, we expanded on our characterization of responses to BDNF by defining “signaling signatures” based on input from all measured signaling markers without regard to cell type.

To move beyond separate analysis of individual markers, we performed unsupervised Leiden clustering based exclusively on signaling marker abundance, agnostic to cell identity (Fig. 4A). This re-clustering analysis resolved 21 signaling clusters (fig. S9A) distinguished by their marker expression profiles (fig. S9B). By plotting cells back onto the generated signaling UMAP by time and treatment, we were able to observe shifts in the distribution of cells to define signaling signatures. Based on the shift in distribution upon BDNF stimulation (Fig. 4B), we identified three temporal signaling signatures – Signature A (rapid pAkt/pERK), Signature B (sustained pS6), and Signature C (complex multi-marker activation) – as well as Basal and Non-Signaling Signatures (Fig. 4C). Of the 21 signaling clusters identified by the clustering analysis, 13 were represented in these defined signaling signatures, each exhibiting a unique signaling marker expression profile (Fig. 4D).

Surprisingly, when we mapped cell types back onto the signaling UMAP, they grouped together, even without identity markers in the input data (Fig. 4E). When we plotted the distribution of individual cell types over time, each followed a unique temporal profile. Intermediate neurons progressed primarily through Signature B, whereas mature neurons adopted the more complex Signature C (Fig. 4F). Although these temporal snapshots represent population shifts rather than individual cell trajectories, the divergence between mature and intermediate neurons shows that maturation state defines not just the magnitude, but the “signature” of BDNF signal induction. These data suggest that BDNF responsiveness is a programmed feature of cell identity, where different lineages decode the same ligand into unique, temporally regulated signaling signatures (Fig. 4G).

The sustained reduction of surface TrkB correlates with BDNF sensitivity

We next sought to identify the molecular mechanisms governing these distinct signaling signatures. A primary candidate for this variability is the relative abundance of the two BDNF receptors themselves; however, it remains unknown to what degree TrkB and p75NTR density dictate signaling magnitude and pathway specificity across cell populations.

To resolve this, we first quantified the contribution of total TrkB receptor expression using a tiered pseudobulk analysis, where each cell was categorized based on its total level of TrkB (Fig. 5A; “None”, “Lo”, “Med”, “Hi”). While 91.23% of cells express some level of TrkB, receptor density was not a consistent predictor of signaling output (Fig. 5B, fig. S10A). Increased activation of effectors downstream of BDNF-TrkB, such as pERK and pS6, were primarily associated with TrkB presence; however, pCREB was not directly correlated with increased TrkB levels, suggesting TrkB abundance is not the only factor driving its activation (Fig. 5B). Cells not expressing TrkB (“None”) showed no activation of certain signaling markers, such as pNF-kappa-B and p-c-Jun, though this population of cells did exhibit increase in pERK, pS6 and pCREB (Fig. 5B), supporting

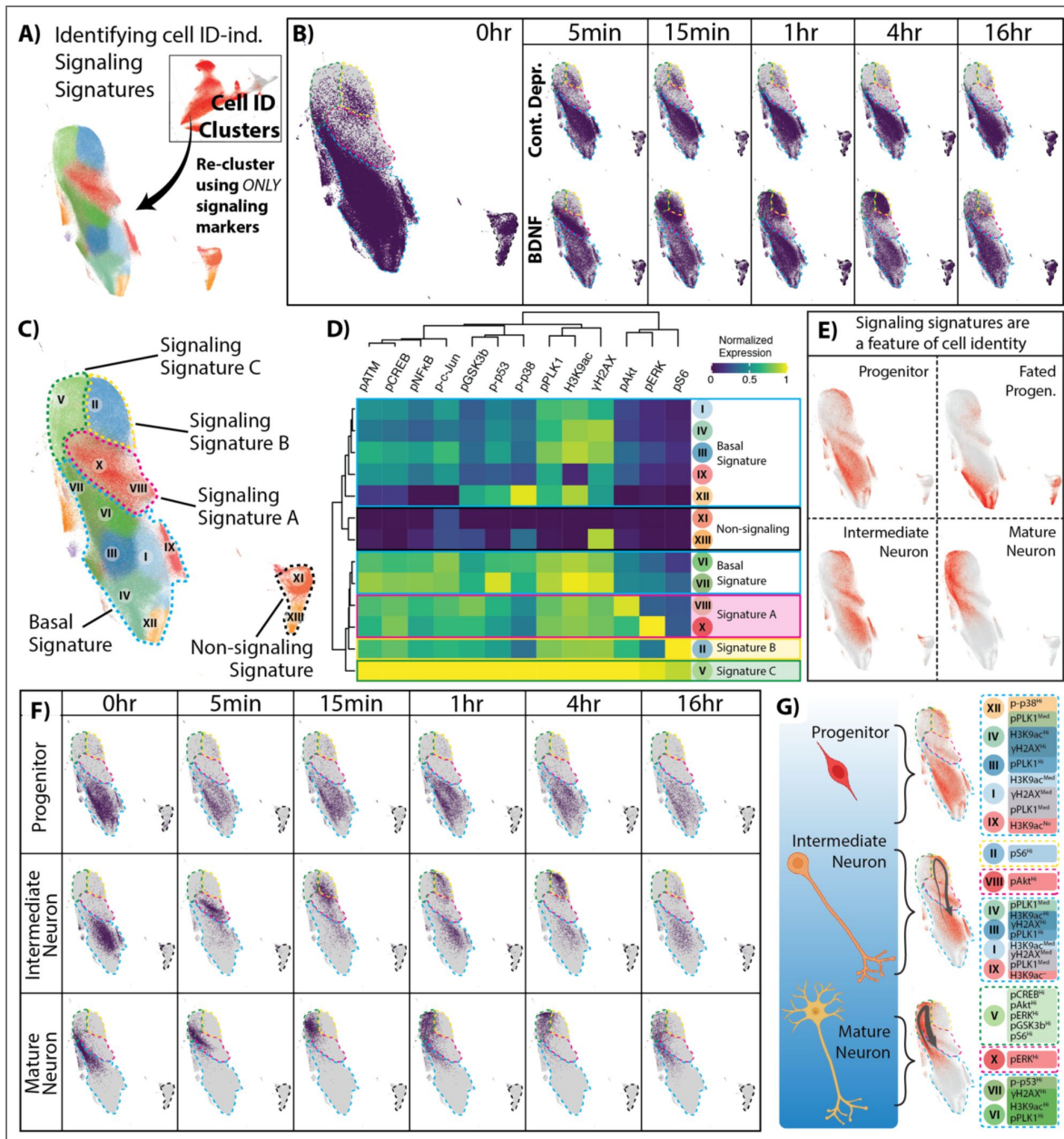


Fig. 4. BDNF induces signaling signature defined by time and by cell type.

(A) Depiction of re-clustering of cell ID clusters (excluding Unassigned) using signaling markers to identify signaling signatures that are agnostic to the initial cell identity. (B) UMAP colored by time point within continued deprivation or BDNF treatment to show the temporal shift in cell distribution across the signaling signature landscape. (C) UMAP of signaling clusters that dynamic shift in cell distribution upon BDNF induction. Signaling clusters are categorized into Non-signaling Signature, Basal Signature, Signaling Signature A, Signaling Signature A, and Signaling Signature C based on the BDNF-induced temporal shifts in distribution. (D) Expression heatmap for indicated signaling clusters to molecularly define the identified signaling signatures. (E) Select cell ID clusters are overlaid on the signaling signature UMAP to identify signaling-driven grouping of cells. (F) UMAP colored by time point across cell types treated with BDNF to depict temporal shift in cell distribution. (G) Signaling dynamics are summarized for selected cell types. Created in *BioRender*.

the established idea that BDNF signaling is not solely mediated through TrkB. Additionally, the increase in pERK in the “None” cell population aligns with our observation that Trk inhibition only partially suppresses ERK activation (Fig. 2C [↗](#)).

To assess whether different levels of TrkB influenced signaling profiles in different cell types, we incorporated TrkB expression level categories into our signaling signature analysis (Fig. 5C [↗](#)). In cell types with robust responses, such as intermediate and mature neurons, all levels of TrkB in the given cell type were present in BDNF-responsive (insets; Signatures A-C) and Basal Signatures (blue dashed outline). Within signaling signatures, there is some grouping based on TrkB level – most notably, TrkB-Hi in mature neurons in Signature C (green dashed outline) – suggesting some contribution of TrkB level to the temporal signaling profile. Although fewer in number, some progenitor cells were present in BDNF-responsive signatures (inset), which had varying levels of TrkB. However, the majority of progenitors exhibit a Basal Signature (blue dashed outline in Fig. 5C [↗](#)), despite harboring Med-to-Hi levels of TrkB (Fig. 5D [↗](#)). This presents an apparent paradox whereby TrkB-expressing cells (i.e. progenitors) can be insensitive to BDNF.

One possible mechanism for the TrkB-high, signaling-silent progenitors is that TrkB in progenitors might not undergo endocytosis, a process thought to be required for BDNF signaling. Using a surface-specific staining protocol, we quantified ligand-induced TrkB depletion from the plasma membrane (Fig. 5E [↗](#)). Our results show a clear correlation between signaling competence and a reduction of surface receptor abundance (Fig. 5F [↗](#)). While intermediate and mature neurons showed significant surface TrkB depletion at later time points, unresponsive progenitors exhibited stable surface profiles. This lack of surface TrkB reduction provides a correlative explanation for why receptor-positive cells remain functionally signaling-silent. These data indicate that the reduction of surface receptors over time is an important part of BDNF regulation (Fig. 5G [↗](#)), suggesting that surface receptor dynamics may serve as a predictor of responsiveness beyond static protein abundance alone.

To assess the contribution of p75NTR expression on BDNF-induced signaling, we performed a tiered pseudobulk analysis based on the level of p75NTR in each cell. Comparison of expression level categories shows an apparent shift in signaling patterns: high p75NTR density was associated with increased stress-responsive p-c-Jun and p38 activation, but also unexpectedly amplified trophic markers like pCREB and pERK (fig. S10B [↗](#)). Taken together, these analyses suggest that receptor presence alone, regardless of density or receptor profile, is insufficient to confer signaling competence, which is predicted by the sustained time-dependent reduction of surface TrkB.

Cell identity modulates signaling response set by receptor stoichiometry

Our results show that the abundance of each BDNF receptor individually contributes to the BDNF response but does not account for all observed signaling changes. This is expected, as others have established that interplay between TrkB and p75NTR can tune signaling responses (7–11). We therefore wanted to understand how receptor stoichiometry influences the profile of BDNF-induced signaling.

To address this question, we first compared signaling responses in cells with different combinations of TrkB and BDNF. By plotting the level of p75NTR vs total TrkB expression, we were segmented four categories of cells based on our previously-applied tiered pseudobulk analysis: p75NTR–/TrkB–, p75NTR+/TrkB–, p75NTR–/TrkB+ and p75NTR+/TrkB+ (Fig. 6A [↗](#)). Consistent with synergistic models, we observed that TrkB and p75NTR act in concert to amplify markers like pERK, pS6, pCREB, and pNF-kappa-B, while p75NTR expression alone – in the absence of TrkB – was sufficient to drive p-c-Jun activity (Fig. 6B [↗](#), fig. S11 [↗](#)).

We next asked how receptor expression levels influence BDNF-induced signaling responses within a given cell type. Using astrocytes as an example, we observe synergistic amplification of certain signaling markers, where p75NTR+/TrkB+ astrocytes exhibited high activation of pERK and pS6 with a milder increase in pAkt (fig. S12 [↗](#)). Other signaling marker activity did not show synergy:

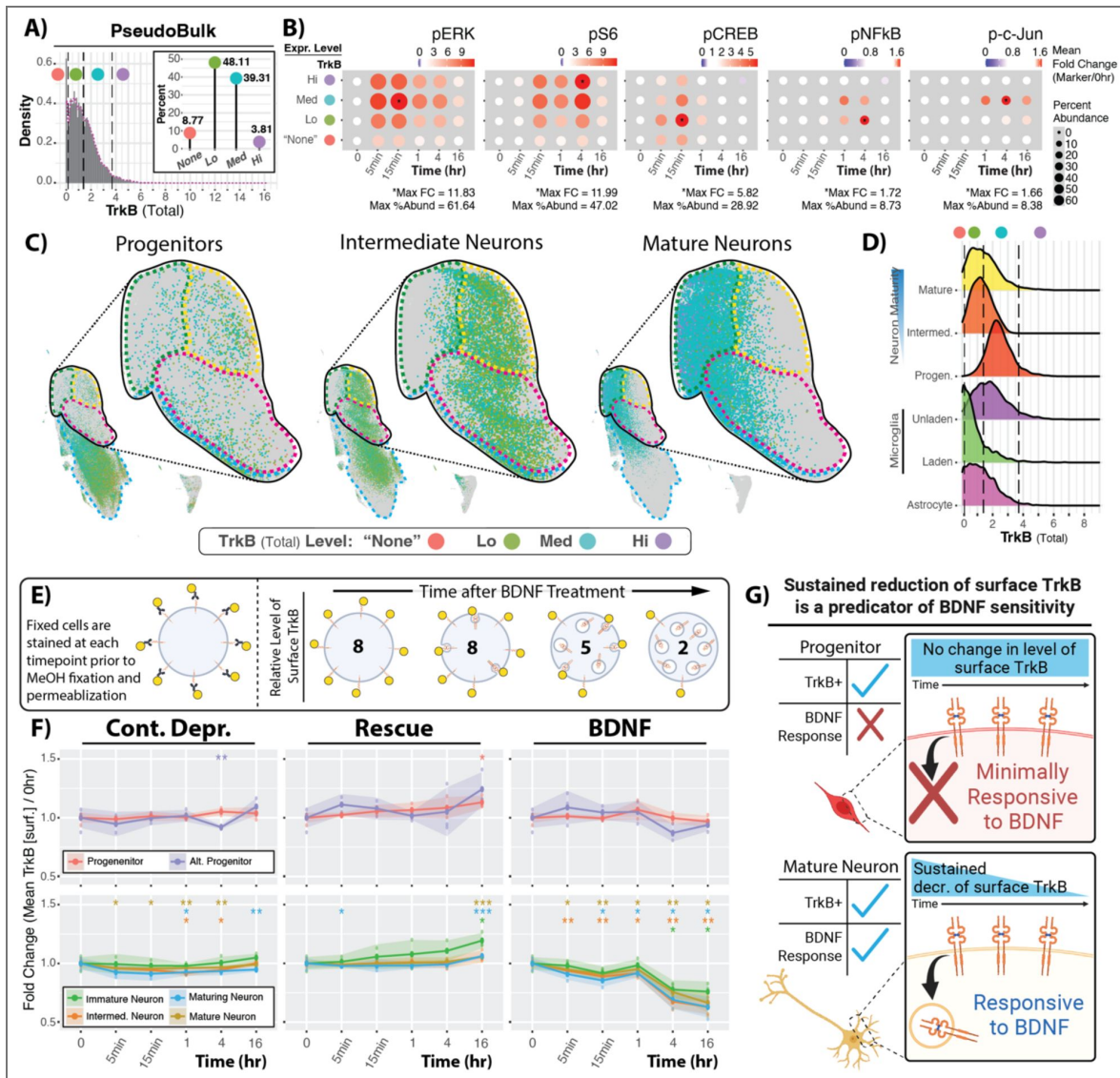


Fig. 5. TrkB internalization defines subpopulations exhibiting distinct signaling patterns within the same cell type.

(A) Distribution and categorization of TrkB (total) expression level in pseudobulk data. Inset depicts percent of all cells within each expression category. (B) Pseudobulk signaling response within each expression category to define general trends correlating to TrkB expression. (C) Distribution of signaling signatures by cell ID and colored by TrkB (total) expression levels. Dotted lines indicate Signaling Signature A (rapid pAkt/pERK; magenta), B (sustained pS6; yellow), and C (complex multi-marker activation; green). Insets highlight the BDNF-induced signatures. (D) TrkB (total) expression distribution across selected cell types, indicating each cell type expresses some degree of TrkB. Dashed lines represent the same values set on pseudobulk data in (A). (E) Diagram of TrkB surface staining used as a proxy to measure TrkB internalization. (F) Temporal trend of TrkB (surface) in response to continued deprivation (Cont. Depr.), Rescue, or BDNF within select cell types. Individual points represent the fold change of the mean of each replicate (0hr, n = 4; Cont. Depr., n = 2-3; Rescue, n = 2-3; BDNF, n = 3) and summarized by mean ± SD. p-values are relative to the 0hr samples, colored by cell type, and determined by unpaired Student t test (* p < 0.05; ** p < 0.01; *** p < 0.001). (G) Results suggest that surface dynamics of TrkB is a better predictor of BDNF responsiveness than static TrkB abundance. Created in *BioRender*.

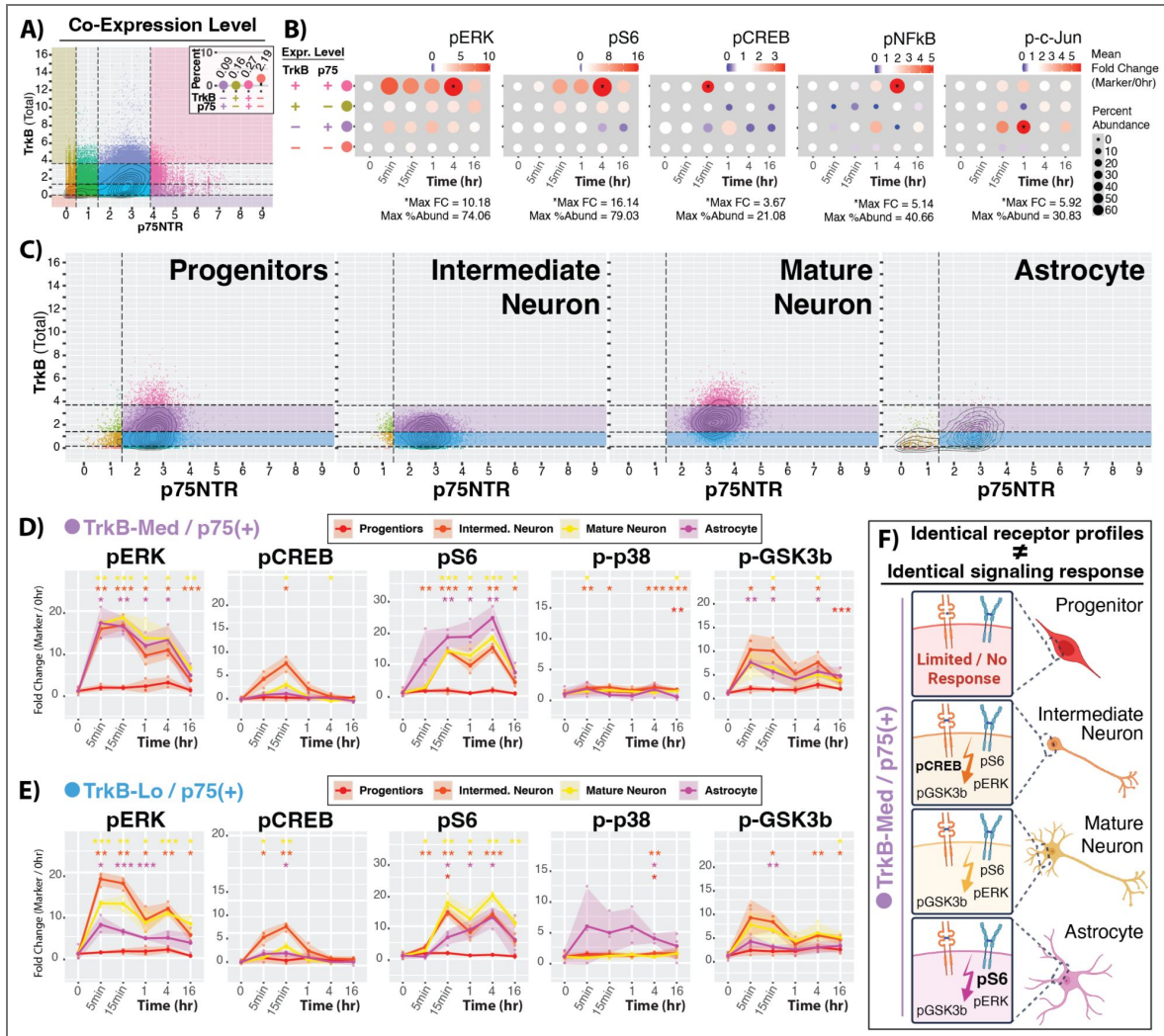


Fig. 6. Identical BDNF receptor profiles do not confer identical responses across cell types.

(A) Distribution and categorization of TrkB and p75NTR expression level in pseudobulk data. Inset depicts percent of all cells within select expression categories defining TrkB⁻/p75⁻, TrkB⁻/p75⁺, TrkB⁺/p75⁻, TrkB⁺/p75⁺ subpopulations. (B) Pseudobulk signaling response within each expression category highlighted in (A) to define general trends correlating to TrkB, p75NTR co-/expression. (C) Distribution and categorization previously characterized cell types based on TrkB, p75NTR co-/expression. (D, E) Comparison of signaling dynamics across cell types with a (D) TrkB-Med/p75⁺ or (E) TrkB-Med/p75⁺ expression pattern. (F) Schematic depicting cells with the same BDNF receptor profile exhibiting different signaling responses. Created in *BioRender*. (D-E) Individual points indicate replicate values (0hr, n = 4; BDNF, n = 3) and summarized by mean±SD; p-values are relative to the 0hr samples, colored by cell type, and determined by unpaired Student t test (* p < 0.05; ** p < 0.01; *** p < 0.001).

pGSK3b exhibited similar responses in TrkB-med cells regardless of p75NTR presence, and p-p53 was only increased in p75NTR⁻/TrkB-med, suggesting a TrkB-dependent/p75NTR-independent response. Together, this analysis shows that receptor stoichiometry can influence BDNF-induced signaling in the same cell type.

To determine if receptor expression level is the ultimate determinant of signaling output, we the analyzed signaling responses across different cell types, holding the receptor expression profile constant. We isolated subpopulations of astrocytes, progenitors, intermediate neurons, and mature neurons that were matched for identical surface levels of both TrkB and p75NTR (Fig. 6C). Surprisingly, an identical receptor profile (for instance TrkB-med/p75(+)) did not result in an identical response. Instead, each cell type produced distinct signaling patterns (Fig. 6D). This observation held when comparing cell-type specific responses in a different receptor profile (TrkB-lo/p75(+); Fig. 6E, fig. S13). Additional comparison of the same cell type across these two receptor profiles highlights our observation that receptor stoichiometry can modulate signaling responses.

However, these results ultimately demonstrate that while receptors are necessary for BDNF responsiveness, they are not sufficient to dictate the signaling pattern (Fig. 6F). Instead, the receptor stoichiometry sets the potential of BDNF sensitivity, which is further tuned by lineage-dependent regulators. These observations suggest that BDNF signaling is a hierarchical process whereby the cell's internal state determines the signaling outcome of this single extracellular cue.

Discussion

The signaling response to BDNF is traditionally understood through receptor biology. Our results support a more holistic model in which receptor stoichiometry sets the potential for BDNF sensitivity, and the intrinsic environment allows for a cell to engage that potential. By moving beyond the “average” signals of bulk biochemistry, our high-dimensional analysis reveals a BDNF-induced signaling landscape where identical receptor profiles produce differing signaling patterns across various cell types. By reframing BDNF sensitivity as a form of prepared competence, we can view BDNF-induced signaling as interconnected points of regulation (Fig. 7). While receptor stoichiometry primes a cell to respond to BDNF, additional factors – such as surface receptor dynamics – that are intrinsic to individual cell types determine exactly when and how the BDNF message is translated into a functional outcome.

Cell type-specific context defines BDNF response set by receptor stoichiometry

A prevailing assumption of receptor-ligand signaling posits that receptor ratio and density completely predict signaling outcomes. However, by isolating subpopulations with matched receptor expression patterns across unique lineages, we demonstrate that this model is incomplete. To our surprise, identical receptor profiles yielded largely different signaling programs across cell types: a mature neuron's response is fundamentally different from that of an astrocyte or progenitor even at the same TrkB/p75 stoichiometries. This indicates that the interpretation of a BDNF signal is not invariantly set by the receptor stoichiometry itself but is modulated by the intracellular context. Our results expand upon computational models of NGF/TrkA signaling which suggest that protein expression noise – specifically intrinsic noise (15, 16) – drives single-cell ERK variability (12, 17). Furthermore, our multiplexed measurements provide a concrete example of a biological context that sets the 'cell state' described in these models: the extent of neuronal differentiation sets a maturation gradient with distinct BDNF responsiveness. This suggests that previously observed stochastic variance may actually reflect programmed, deterministic differences across neuronal maturity, thus reframing 'noise' as a developmentally regulated feature.

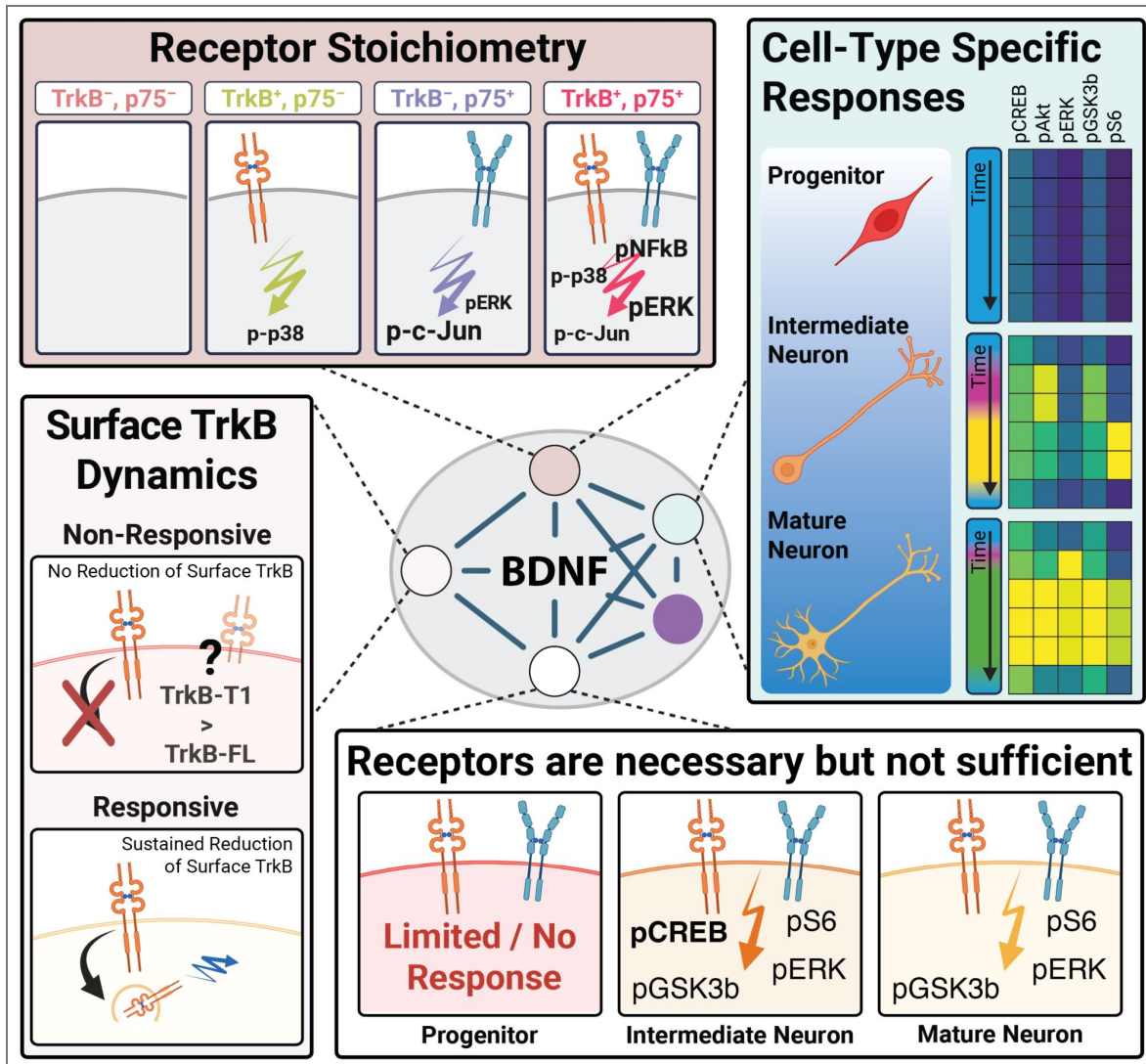


Fig. 7. Factors contributing to the heterogeneity of BDNF signaling responses.

Stimulation with BDNF induces different cell signaling responses across different cell types. The pattern of BDNF receptor abundance is necessary to regulate how cells respond; however, stoichiometry alone is not sufficient to explain how some cell types are non-responsive, despite high levels of TrkB. A better predictor of BDNF sensitivity is the prolonged reduction of surface TrkB receptor (i.e. internalization), where the ratio of TrkB isoforms may add a level of developmental competency to the overall regulation network. Ultimately, the cell-intrinsic environment acts as the final filter through which a cell interprets the BDNF message. Created in *BioRender*.

Sustained reduction of surface TrkB is a functional correlate of responsiveness

If receptor density cannot predict signaling output, does receptor trafficking serve as the primary indicator of responsiveness? Following ligand binding, TrkB is internalized into signaling endosomes to trigger canonical trophic cascades (6, 18). Our data indicate a correlation between signaling competence and receptor trafficking: while neurons and astrocytes show significant ligand-induced surface TrkB depletion, non-responsive populations – most notably progenitors – exhibit stable surface receptor levels. Similar to other signaling systems modulated by receptor internalization (19), our observation suggests a trafficking-based explanation for why receptor-positive cells remain signaling-silent. While these findings are correlative and do not yet prove a causal requirement for internalization, the consistency of this pattern across neural lineages suggests that trafficking kinetics are a more reliable predictor of BDNF sensitivity than static protein abundance. Defining the precise molecular regulators of this internalization at single-cell resolution remains a key open question to be addressed by future endocytic perturbation studies. Furthermore, the progenitor “paradox” (i.e. high TrkB expression paired with negligible internalization) may represent a point of signaling regulation rather than an inability to respond. In this context, progenitor non-responsiveness could be a mechanism of “prepared competence,” where cells maintain a high TrkB density as they await a developmental window that permits differentiation. A compelling candidate for this gate is a developmental switch from truncated (TrkB-T1) to full-length (TrkB-FL) isoform expression. Under this hypothesis, TrkB-T1 would act as a signaling sink or dominant-negative regulator (20, 21) until TrkB-FL expression becomes dominant, which would have profound consequences for progenitor cell-fate decisions (22, 23). Although our antibody targets the shared extracellular domain and cannot discern these isoforms, our data are consistent with this hypothesized cell-intrinsic factor due to the presence of the receptor but a lack of sustained surface reduction and signaling response. Thus, further investigation is warranted into this potential mechanism of prepared competence.

Receptors are necessary, but not sufficient in BDNF signaling regulation

While receptor trafficking provides a rationalization of BDNF responsiveness, how does the interplay between TrkB and p75NTR shape BDNF signaling? Our results suggest that BDNF pathways utilize a combinatorial logic where the level of receptor availability tunes specific cascades. Consistent with established synergistic models (7, 9, 21, 22), we observe that TrkB and p75NTR act synergistically to amplify trophic pathways like pERK and pNF-kappa-B, while p75NTR alone is sufficient to drive stress-responsive p-c-Jun activity. We posit that these patterns may be further regulated by p75NTR cleavage dynamics (23), adding another layer of receptor-mediated regulation. This high-resolution mapping highlights that p75NTR is not merely a “death receptor” but a critical synergistic partner that heightens cellular sensitivity to the BDNF message in the context of our experimental system.

It is unsurprising that receptors are necessary to initiate BDNF-induced signaling; however, our results indicate that receptor presence alone is not sufficient to dictate the final output. We demonstrate that this receptor interplay is modulated by cellular context unique to each lineage. This is evidenced by our finding that equivalent receptor expression patterns yield varying signaling programs (Fig. 6 [↗](#)), that only a discrete subpopulation (~47–75%) of total cells respond to BDNF stimulation (Fig. 2 [↗](#)), and that unsupervised clustering based solely on signaling markers independently groups cells by their biological identity (Fig. 2 [↗](#)).

Intrinsic factors ultimately gate BDNF interpretation across distinct cell types

While we cannot determine from fixed data whether individual cells traverse signaling signatures sequentially or preferentially occupy different signatures, insights from these data – made possible through high-dimensional single-cell proteomics – suggest a hierarchy of filters. These intrinsic filters may include receptor isoform ratio (20, 21), cleavage and internalization dynamics (23), cell cycle phase (24), or the epigenetic landscape (25–27), which likely determines the accessibility of target genes for BDNF-induced expression. Such multifactorial logic – where the signaling pattern rather than amplitude encodes biological meaning – mirrors findings in other systems, including calcium oscillations (28–31), TNF-NF-kappa-B dynamics (32–34), Notch signaling (35), growth factor-induced PI3K activity (36), and Wnt signaling (37, 38). By demonstrating that lineage modulates stoichiometry, we reframe BDNF signaling as a tiered process where maturation state defines the functional meaning of the extracellular cue.

While our high-dimensional approach provides a new framework for understanding BDNF signaling, several limitations of the current study warrant consideration. First, our findings regarding TrkB internalization and downstream signaling remain primarily correlative. Although the lack of receptor trafficking in progenitors serves as a consistent predictor of signaling silence, future investigation is required to establish a direct causal requirement for internalization in this specific context. Second, our analysis relies on discrete temporal snapshots. While these timepoints capture the evolution of signaling signatures across the population, they cannot directly track the dynamic trajectories of individual cells as they transition between signaling states. Furthermore, our findings are derived from an *in vitro* primary culture system; while this allowed for the high-resolution mapping of endogenous spinal cord lineages, future studies are required to determine how these nodes of regulation are modulated within the complex three-dimensional environment of the *in vivo* niche. Finally, our use of an antibody targeting the shared extracellular domain of TrkB introduces ambiguity regarding receptor isoforms. While we hypothesize that the “progenitor paradox” may be driven by a developmental switch between truncated (TrkB-T1) and full-length (TrkB-FL) isoforms, definitive confirmation of this “active gate” will require the development of isoform-specific proteomic probes. Addressing these limitations through targeted genetic perturbations will be essential to further validating the multi-layered model of neurotrophin regulation suggested here. Additionally, our study exclusively examines the response to mature BDNF. Because proBDNF preferentially engages p75NTR rather than TrkB (39–41), comparing the signaling landscapes elicited by each ligand form would directly test whether the regulatory nodes we describe are reconfigured when the receptor entry point shifts from TrkB to p75NTR, potentially identifying an additional layer of ligand-form-dependent route diversity.

Beyond fundamental signaling, these findings suggest a new logic for neurotrophic drug development for neurological diseases and disorders. Our model predicts that global TrkB agonists will exhibit cell-type-specific efficacy *in vivo*, potentially explaining the inconsistent results and partial success of BDNF-based therapies in clinical trials (42, 43). Effective strategies must likely move beyond simple receptor agonism toward combination approaches that shift the intracellular context – transitioning a cell from a signaling-silent state to a BDNF-sensitive one. For example, the use of maturation-stage-specific HDAC inhibitors could remodel the epigenetic landscape of stagnant populations (25, 44), lowering the “intrinsic filter” to permit TrkB-mediated differentiation. However, the transition *in vivo* faces the formidable challenge of cell-type-specific delivery (43), as ensuring context-shifting agents reach the intended subpopulation without inducing off-target effects in already-responsive neurons remains a hurdle. Ultimately, this study suggests that neurotrophin sensitivity is a form of prepared competence that lies not just in the ligand and the receptors, but in the internal machinery of the cell itself.

Materials and methods

1. Animals

All experiments were conducted in accordance with AAALAC guidelines on a protocol approved by the University of Virginia ACUC. Timed pregnant Sprague Dawley rats were purchased from Charles River (Strain Code: 001) at embryonic day 12 (E12) and housed on a 12hr light/dark cycle prior to embryonic tissue dissection.

2. Cell culture

Primary dissociated neural cultures were prepared from E14 Sprague Dawley rat spinal cords. Briefly, spinal cords (sacral level excluded) were dissected in chilled HBSS, minced, and enzymatically digested for 15 min at 37°C in a filtered enzyme solution containing 0.25% (w/v) trypsin, 0.04% (w/v) hyaluronidase, and 0.04% (w/v) DNase. Tissue was mechanically dissociated by trituration in plating media (Basal Medium Eagle supplemented with 5% FBS, 1X N2 Supplement, 1X GlutaMAX, and 1% Penicillin-Streptomycin) and passed through a 70 µm cell strainer. Cells were plated at a density of 5×10⁵ cells/well in 12-well plates pre-coated with 0.1 mg/mL poly-D-lysine (overnight) and 15 µg/mL laminin (>2hr) in PBS. Initial cell viability was >90% as determined by Trypan blue exclusion prior to plating. Within 16hrs, plating media was replaced with Maintenance Media (Neurobasal media supplemented with 1X B27 and 1X GlutaMAX). Cultures were maintained at 37°C in 5% CO₂, with half-volume media exchanges every 48hrs.

At day in vitro (DIV) 3.5, cultures were washed three times with a working volume (0.5mL) of Deprivation Media (Neurobasal and 1% Penicillin-Streptomycin) and deprived of trophic support for 12hrs prior to treatment. Cells were then stimulated with 50 ng/mL BDNF (9), 200 nM K252a (45, 46), or a combination in deprivation media for specified durations (5min to 72hrs). Maintenance Media was used as a Rescue positive control, while fresh Deprivation Media was applied to the Continued Deprivation negative control.

3. Mass cytometry sample collection

Following stimulation, treatment media was replaced with 500 µL of room-temperature Accutase. Cells were monitored for detachment, mechanically dissociated via P1000 trituration into a single-cell suspension, and filtered through a 70 µm strainer into 500 µL of 4% paraformaldehyde (PFA) in PBS. Total processing time from media removal to fixation was maintained under 90s to preserve transient signaling states as best as possible. After a 10 min fixation at room temperature, cells were pelleted (500*g, 5 min), resuspended in 500 µL of Cell Storage Media (CSM; DPBS with 0.5% w/v BSA and 0.2% w/v sodium azide), and aliquoted for quality control and cell counting. Samples were stored at -80°C until analysis.

Each biological replicate (n) represents a neural culture generated from an independent timed-pregnant litter. To ensure statistical robustness and account for batch effects, treatments were collected with 2-4 biological replicates per time point (table S2 4), with BDNF-treated samples (5min to 16hr) performed in triplicate and baseline (0hr) controls in quadruplicate.

4. Sample barcoding, staining, and mass cytometry

Samples were stained according to established high-dimensional mass cytometry protocols (47–51). To minimize inter-sample staining variability and mitigate batch effects, individual samples were uniquely barcoded using a “6-choose-3” combinatorial system of palladium metals (52, 53). To account for potential inter-run variations across barcoded batches, a “universal reference” sample – comprising pooled aliquots (11µL, ~2.44%) of all experimental samples pooled – was included in every barcode set. Barcoding was achieved through reversible permeabilization in 0.02% saponin for 15 min at room temperature with agitation (54).

Following barcoding, samples were pooled and blocked with 10% Normal Donkey Serum in CSM for 30min. Cells were first stained for 30min with a primary antibody cocktail targeting extracellular epitopes, including the TrkB extracellular domain that enabled our assessment of surface TrkB dynamics (table S1 [↗](#)). Samples were then fixed and permeabilized with ice-cold 100% methanol for 10min, with vortexing every 2min to prevent cell clumping. Permeabilized cells were subsequently stained for 1hr with a cocktail of antibodies against intracellular targets (table S1 [↗](#)). To distinguish single-cell events from debris, samples were incubated overnight at 4°C in 1.6% PFA/DPBS containing 125 µM Iridium (Ir)-intercalator (Standard Biotech, South San Francisco, CA). Prior to analysis, pooled samples were resuspended in Maxpar Cell Acquisition Solution (CAS) Plus and filtered through a 40µm strainer. Data were acquired on a Helios CyTOF XT system (Standard Biotech) at an acquisition rate below 500 events per second. Samples were processed in four sequential batches of 20 barcoded samples each (table S2 [↗](#)). Data were collected using Helios CyTOF.

5. Normalization, debarcoding, and single cell gating

Raw FCS files were standardized via bead-based normalization to account for instrument sensitivity fluctuations (55). Samples were then debarcoded using a “6-choose-3” combinatorial system to assign events to their respective biological replicates (53). To ensure high data quality for the resulting dataset, single-cell events were isolated through a standardized cleanup gating strategy in Cytobank.

Events were first filtered by low barcode separation distance and high Mahalanobis distance to remove poorly assigned cells. Singlets were isolated by comparing event center to event length and width. Residual EQ calibration beads were excluded by gating out high cerium (Ce140) events, while environmental contaminants (Sn120, I127, Cs133, Ba138, Pb208) were identified and removed by gating against the Iridium DNA intercalator (Ir191/193). A specific gate on Gd157 was applied to eliminate bleed-through signal from Nd141. The resulting high-fidelity 680,000-cell dataset of single-cell events were exported as individual FCS files per sample for downstream analysis (<https://community.cytobank.org/cytobank/experiments/121988> [↗](#)).

6. Batch correction

To account for potential batch effects, data from the “universal reference” sample included in each barcode batch were used to normalize signal intensities across batches using a quantile-based adjustment method (<https://github.com/CUHIMSR/CytofBatchAdjust> [↗](#); R-4.5.2) (56). This approach effectively minimized technical variance (batch effects) while preserving biological heterogeneity across the longitudinal dataset. Although 72hr samples were collected and processed through the batch correction, they were not included in downstream analyses in the present study due to the possibility of post-treatment secretion of growth factors confounding our interpretation of results.

7. Leiden clustering and UMAP visualization

Single-cell events were partitioned into molecularly defined subpopulations using the Leiden community detection algorithm (Python 3.12.4) (49, 57, 58). We employed a two-stage clustering strategy to decouple biological identity from signaling state. First, cells were clustered using lineage-specific ID markers (table S1 [↗](#)) to define cell-type identities (Fig. 1B [↗](#), fig. S1 [↗](#)). Second, to identify unsupervised signaling signatures (Fig. 4 [↗](#)), events – excluding those classified as ‘Unassigned’ – were re-clustered based solely on phosphoprotein markers without a priori identity information. Lineage assignments were subsequently mapped back to signaling clusters using unique event identifiers to determine the cell-type composition of each signature.

High-dimensional data were dimensionally reduced and visualized via Uniform Manifold Approximation and Projection (UMAP) (59, 60) using the following parameters: nearest neighbors = 15, metric = Euclidean, local connectivity = 1, epochs = 1000. All UMAP visualizations were generated in R-4.5.2.

8. Data analysis and quantification

Pre-processed mass cytometry data were analyzed using custom R (R-4.5.2) scripts. To quantify signaling induction across the heterogeneous population, we defined a “signaling response” as any event exceeding the 95th percentile of the baseline signal intensity observed in the 0-hour (trophic-deprived) control for each respective phosphoprotein. This thresholding was applied globally and, where indicated, to individual cell-type clusters to account for lineage-specific baseline variances (fig. S2 [↗](#)).

Responsiveness was quantified as percent abundance, representing the proportion of “responsive” cells relative to the total population within a given treatment condition or cell-type cluster. For stoichiometry analysis, receptor expression tiers (“None”, “Lo”, “Med”, “Hi”) were established via logical biaxial gating of total TrkB and p75NTR across the entire dataset. This tiered approach allowed for the identification of the “progenitor paradox” and supported the finding that receptor density alone is an unreliable predictor of signaling output. All custom analysis scripts and data processing pipelines are available at <https://github.com/TooSewellForSkool/Sewell-et-al-BDNF-Signaling-Manuscript> [↗](#).

9. Statistics

Data are presented as mean±SD. Each biological replicate (n) represents a neural culture derived from an independent timed-pregnant litter. For comparisons between two groups, an unpaired two-tailed Student’s t-test was performed compared to 0hr. All statistical analyses were conducted using R-4.5.2, and an alpha level of $p < 0.05$ was considered statistically significant.

Data availability

Raw FCS files are available at <https://community.cytobank.org/cytobank/experiments/121988> [↗](#). All custom analysis scripts and data processing pipelines are available at <https://github.com/TooSewellForSkool/Sewell-et-al-BDNF-Signaling-Manuscript> [↗](#).

Additional files

Supplementary material [↗](#) Fig. S1 [↗](#). Characterization of cell identity clusters and their distribution. Fig. S2 [↗](#). Defining the cells that are responsive to treatment. Fig. S3 [↗](#). Comparison of different threshold cutoffs and different treatments. Fig. S4 [↗](#). BDNF-induced responses and the effect of K252A inhibition – Extension of Fig. 2B, C [↗](#). Fig. S5 [↗](#). Pseudobulk signaling response to rescue and BDNF treatment. Fig. S6 [↗](#). BDNF-induced signaling changes in Neuronal and Non-Neuronal cell categories. Fig. S7 [↗](#). BDNF-induced signaling across distinct cell types – Extension of Fig. 3B, F [↗](#). Fig. S8 [↗](#). Comparison of signaling responses across treatments in neuronal lineage cell types. Fig. S9 [↗](#). Signaling signatures agnostic to cell ID clustering information. Fig. S10 [↗](#). BDNF receptor level contribution to pseudobulk signaling response. Fig. S11 [↗](#). Pseudobulk analysis of receptor level contribution to signaling heterogeneity. Fig. S12 [↗](#). Receptor expression level contributes to signaling heterogeneity within the same cell type – Extension of Fig. 6B [↗](#). Fig. S13 [↗](#). Signaling comparison of different cell types with the same receptor profile – Extension of Fig. 6D, E [↗](#). Table S1 [↗](#). Mass cytometry antibody panel. Table S2 [↗](#). Sample organization into barcode sets. Table S3 [↗](#). p-values for statistics performed in Fig. 2C [↗](#) and Fig. S4B [↗](#). Table S4 [↗](#). p-values for statistics performed in Fig. 3 [↗](#).

Additional information

Funding

Funder	Grant reference number	Author
HHS National Institutes of Health (NIH)	F31NS135970	Jonathon M Sewell
HHS National Institutes of Health (NIH)	T32GM139787	Jonathon M Sewell

HHS National Institutes of Health (NIH)	R01NS111220	Eli R Zunder
HHS National Institutes of Health (NIH)	R01NS083378	Bettina Winckler
HHS National Institutes of Health (NIH)	R01NS136342	Christopher D Deppmann
UV Brain Institute, University of Virginia (UVA Brain Institute)	Presidential Fellowship in Collaborative Neuroscience	Jonathon M Sewell

Author ORCID iDs

Jonathon M Sewell:  <https://orcid.org/0000-0002-2597-646X>

Chris D Deppmann:  <https://orcid.org/0000-0002-6591-1767>

References

- Kowiański P**, Lietzau G, Czuba E, Waśkow M, Steliga A, Moryś J (2018) BDNF: A Key Factor with Multipotent Impact on Brain Signaling and Synaptic Plasticity. *Cell. Mol. Neurobiol* **38**:579-593 <https://doi.org/10.1007/s10571-017-0510-4> | PubMed
- Huang EJ**, Reichardt LF (2001) Neurotrophins: roles in neuronal development and function. *Annu. Rev. Neurosci* **24**:677-736 <https://doi.org/10.1146/annurev.neuro.24.1.677> | PubMed
- Miranda-Lourenço C**, Ribeiro-Rodrigues L, Fonseca-Gomes J, Tanqueiro SR, Belo RF, Ferreira CB, Rei N, Ferreira-Manso M, de Almeida-Borlido C, Costa-Coelho T, *et al.* (2020) Challenges of BDNF-based therapies: From common to rare diseases. *Pharmacol Res* **162** <https://doi.org/10.1016/j.phrs.2020.105281> | PubMed
- Wang CS**, Kavalali ET, Monteggia LM (2022) BDNF signaling in context: From synaptic regulation to psychiatric disorders. *Cell* **185**:62-76 <https://doi.org/10.1016/j.cell.2021.12.003> | PubMed
- Hernández-Del Caño C**, Varela-Andrés N, Cebrián-León A, Deogracias R (2024) Neurotrophins and their receptors: bdnf's role in gabaergic neurodevelopment and disease. *Int. J. Mol. Sci* **25** <https://doi.org/10.3390/ijms25158312> | PubMed
- Zheng J**, Shen W.-H, Lu T.-J, Zhou Y, Chen Q, Wang Z, Xiang T, Zhu Y.-C, Zhang C, Duan S, *et al.* (2008) Clathrin-dependent endocytosis is required for TrkB-dependent Akt-mediated neuronal protection and dendritic growth. *J. Biol. Chem* **283**:13280-13288 <https://doi.org/10.1074/jbc.m709930200> | PubMed
- Bibel M**, Hoppe E, Barde YA (1999) Biochemical and functional interactions between the neurotrophin receptors trk and p75NTR. *EMBO J* **18**:616-622 <https://doi.org/10.1093/emboj/18.3.616> | PubMed
- Meeker RB**, Williams KS (2015) The p75 neurotrophin receptor: at the crossroad of neural repair and death. *Neural Regen. Res* **10**:721-725 <https://doi.org/10.4103/1673-5374.156967> | PubMed
- Zanin JP**, Montroull LE, Volosin M, Friedman WJ (2019) The p75 neurotrophin receptor facilitates trkb signaling and function in rat hippocampal neurons. *Front. Cell. Neurosci* **13** <https://doi.org/10.3389/fncel.2019.00485> | PubMed
- Conroy JN**, Coulson EJ (2022) High-affinity TrkA and p75 neurotrophin receptor complexes: A twisted affair. *J. Biol. Chem* **298** <https://doi.org/10.1016/j.jbc.2022.101568> | PubMed
- Makkerh JPS**, Ceni C, Auld DS, Vaillancourt F, Dorval G, Barker PA (2005) p75 neurotrophin receptor reduces ligand-induced Trk receptor ubiquitination and delays Trk receptor internalization and degradation. *EMBO Rep* **6**:936-941 <https://doi.org/10.1038/sj.embor.7400503> | PubMed
- Loos C**, Moeller K, Fröhlich F, Hucho T, Hasenauer J, Hierarchical A (2018) Data-Driven Approach to Modeling Single-Cell Populations Predicts Latent Causes of Cell-To-Cell Variability. *Cell Syst* **6**:593-603.e13 <https://doi.org/10.1016/j.cels.2018.04.008> | PubMed
- Birtwistle MR**, Rauch J, Kiyatkin A, Aksamitiene E, Dobrzyński M, Hoek JB, Kolch W, Ogunnaike BA, Kholodenko BN (2012) Emergence of bimodal cell population responses from the interplay between analog single-cell signaling and protein expression noise. *BMC Syst Biol* **6** <https://doi.org/10.1186/1752-0509-6-109> | PubMed

14. Spitzer MH, Nolan GP (2016) Mass cytometry: single cells, many features. *Cell* **165**:780-791 <https://doi.org/10.1016/j.cell.2016.04.019> | PubMed
15. Elowitz MB, Levine AJ, Siggia ED, Swain PS (2002) Stochastic gene expression in a single cell. *Science* **297**:1183-1186 <https://doi.org/10.1126/science.1070919> | PubMed
16. Balázsi G, van Oudenaarden A, Collins JJ (2011) Cellular decision making and biological noise: from microbes to mammals. *Cell* **144**:910-925 <https://doi.org/10.1016/j.cell.2011.01.030> | PubMed
17. Hasenauer J, Hasenauer C, Hucho T, Theis FJ (2014) ODE constrained mixture modelling: a method for unraveling subpopulation structures and dynamics. *PLoS Comput. Biol* **10**:e1003686 <https://doi.org/10.1371/journal.pcbi.1003686> | PubMed
18. Moya-Alvarado G, Tiburcio-Felix R, Ibáñez MR, Aguirre-Soto AA, Guerra MV, Wu C, Mobley WC, Perlson E, Bronfman FC (2023) BDNF/TrkB signaling endosomes in axons coordinate CREB/mTOR activation and protein synthesis in the cell body to induce dendritic growth in cortical neurons. *eLife* **12** <https://doi.org/10.7554/eLife.77455> | PubMed
19. Salavessa L, Lagache T, Malardé V, Grassart A, Olivo-Marin J.-C, Canette A, Trichet M, Sansonetti PJ, Sauvonnnet N (2021) Cytokine receptor cluster size impacts its endocytosis and signaling. *Proc Natl Acad Sci USA* **118** <https://doi.org/10.1073/pnas.2024893118> | PubMed
20. Dorsey SG, Renn CL, Carim-Todd L, Barrick CA, Bambrick L, Krueger BK, Ward CW, Tessarollo L (2006) In vivo restoration of physiological levels of truncated TrkB.T1 receptor rescues neuronal cell death in a trisomic mouse model. *Neuron* **51**:21-28 <https://doi.org/10.1016/j.neuron.2006.06.009> | PubMed
21. Tessarollo L, Yanpallewar S (2022) Trkb truncated isoform receptors as transducers and determinants of BDNF functions. *Front. Neurosci* **16** <https://doi.org/10.3389/fnins.2022.847572> | PubMed
22. Chao MV, Hempstead BL (1995) p75 and Trk: a two-receptor system. *Trends Neurosci* **18**:321-326 [https://doi.org/10.1016/0166-2236\(95\)93921-j](https://doi.org/10.1016/0166-2236(95)93921-j) | PubMed
23. Vicario A, Kiswa L, Tann JY, Kelly CE, Ibáñez CF (2015) Neuron-type-specific signaling by the p75NTR death receptor is regulated by differential proteolytic cleavage. *J. Cell Sci* **128**:1507-1517 <https://doi.org/10.1242/jcs.161745> | PubMed
24. Urdiales JL, Becker E, Andrieu M, Thomas A, Jullien J, van Grunsven LA, Menut S, Evan GI, Martín-Zanca D, Rudkin BB (1998) Cell cycle phase-specific surface expression of nerve growth factor receptors TrkA and p75(NTR). *J. Neurosci* **18**:6767-6775 <https://doi.org/10.1523/jneurosci.18-17-06767.1998> | PubMed
25. Hsieh J, Nakashima K, Kuwabara T, Mejia E, Gage FH (2004) Histone deacetylase inhibition-mediated neuronal differentiation of multipotent adult neural progenitor cells. *Proc Natl Acad Sci USA* **101**:16659-16664 <https://doi.org/10.1073/pnas.0407643101> | PubMed
26. Ma DK, Marchetto MC, Guo JU, Ming G, Gage FH, Song H (2010) Epigenetic choreographers of neurogenesis in the adult mammalian brain. *Nat. Neurosci* **13**:1338-1344 <https://doi.org/10.1038/nn.2672> | PubMed
27. Koppel I, Timmusk T (2013) Differential regulation of Bdnf expression in cortical neurons by class-selective histone deacetylase inhibitors. *Neuropharmacology* **75**:106-115 <https://doi.org/10.1016/j.neuropharm.2013.07.015> | PubMed
28. Berridge MJ (1997) The AM and FM of calcium signalling. *Nature* **386**:759-760 <https://doi.org/10.1038/386759a0> | PubMed
29. Forostyak O, Forostyak S, Kortus S, Sykova E, Verkhratsky A, Dayanithi G (2016) Physiology of Ca(2+) signalling in stem cells of different origins and differentiation stages. *Cell Calcium* **59**:57-66 <https://doi.org/10.1016/j.ceca.2016.02.001> | PubMed
30. Bootman MD, Bultynck G (2020) Fundamentals of cellular calcium signaling: A primer. *Cold Spring Harb Perspect Biol* **12** <https://doi.org/10.1101/cshperspect.a038802> | PubMed

31. **Saghatelian A** (2023) Calcium signaling as an integrator and decoder of niche factors to control somatic stem cell quiescence and activation. *Febs J* **290**:677-683 <https://doi.org/10.1111/febs.16289> | [PubMed](#)
32. **Hoffmann A**, Levchenko A, Scott ML, Baltimore D (2002) The IkappaB-NF-kappaB signaling module: temporal control and selective gene activation. *Science* **298**:1241-1245 <https://doi.org/10.1126/science.1071914> | [PubMed](#)
33. **Junkin M**, Kaestli AJ, Cheng Z, Jordi C, Albayrak C, Hoffmann A, Tay S (2016) High-Content Quantification of Single-Cell Immune Dynamics. *Cell Rep* **15**:411-422 <https://doi.org/10.1016/j.celrep.2016.03.033> | [PubMed](#)
34. **Bozich ER**, Guo X, Wilson JL, Hoffmann A (2025) A computational workflow for assessing drug effects on temporal signaling dynamics reveals robustness in stimulus-specific NFkB signaling. *PLoS Comput. Biol* **21**:e1013344 <https://doi.org/10.1371/journal.pcbi.1013344> | [PubMed](#)
35. **Guo R**, Han D, Song X, Gao Y, Li Z, Li X, Yang Z, Xu Z (2023) Context-dependent regulation of Notch signaling in glial development and tumorigenesis. *Sci. Adv* **9**:eadi2167 <https://doi.org/10.1126/sciadv.adi2167> | [PubMed](#)
36. **Madsen RR**, Vanhaesebroeck B (2020) Cracking the context-specific PI3K signaling code. *Sci. Signal* **13** <https://doi.org/10.1126/scisignal.aay2940> | [PubMed](#)
37. **Goentoro L**, Kirschner MW (2009) Evidence that fold-change, and not absolute level, of beta-catenin dictates Wnt signaling. *Mol. Cell* **36**:872-884 <https://doi.org/10.1016/j.molcel.2009.11.017> | [PubMed](#)
38. **Cselenyi CS**, Lee E (2008) Context-dependent activation or inhibition of Wnt-beta-catenin signaling by Kremen. *Sci. Signal* **1** <https://doi.org/10.1126/stke.18pe10> | [PubMed](#)
39. **Teng HK**, Teng KK, Lee R, Wright S, Tevar S, Almeida RD, Kermani P, Torkin R, Chen Z.-Y, Lee FS, *et al.* (2005) ProBDNF induces neuronal apoptosis via activation of a receptor complex of p75NTR and sortilin. *J. Neurosci* **25**:5455-5463 <https://doi.org/10.1523/jneurosci.5123-04.2005> | [PubMed](#)
40. **Woo NH**, Teng HK, Siao C.-J, Chiaruttini C, Pang PT, Milner TA, Hempstead BL, Lu B (2005) Activation of p75NTR by proBDNF facilitates hippocampal long-term depression. *Nat. Neurosci* **8**:1069-1077 <https://doi.org/10.1038/nn1510> | [PubMed](#)
41. **Yang F**, Je H.-S, Ji Y, Nagappan G, Hempstead B, Lu B (2009) Pro-BDNF-induced synaptic depression and retraction at developing neuromuscular synapses. *J. Cell Biol* **185**:727-741 <https://doi.org/10.1083/jcb.200811147> | [PubMed](#)
42. (1999) A controlled trial of recombinant methionyl human BDNF in ALS: The BDNF Study Group (Phase III). *Neurology* **52**:1427-1433 <https://doi.org/10.1212/wnl.52.7.1427> | [PubMed](#)
43. **Nagahara AH**, Tuszynski MH (2011) Potential therapeutic uses of BDNF in neurological and psychiatric disorders. *Nat. Rev. Drug Discov* **10**:209-219 <https://doi.org/10.1038/nrd3366> | [PubMed](#)
44. **Schroeder FA**, Lewis MC, Fass DM, Wagner FF, Zhang Y.-L, Hennig KM, Gale J, Zhao W.-N, Reis S, Barker DD, *et al.* (2013) A selective HDAC 1/2 inhibitor modulates chromatin and gene expression in brain and alters mouse behavior in two mood-related tests. *PLoS ONE* **8**:e71323 <https://doi.org/10.1371/journal.pone.0071323> | [PubMed](#)
45. **Perez-Pinera P**, Hernandez T, García-Suárez O, de Carlos F, Germana A, Del Valle M, Astudillo A, Vega JA (2007) The Trk tyrosine kinase inhibitor K252a regulates growth of lung adenocarcinomas. *Mol. Cell. Biochem* **295**:19-26 <https://doi.org/10.1007/s11010-006-9267-7> | [PubMed](#)
46. **Tapley P**, Lamballe F, Barbacid M (1992) K252a is a selective inhibitor of the tyrosine protein kinase activity of the trk family of oncogenes and neurotrophin receptors. *Oncogene* **7**:371-381 [PubMed](#)
47. **Keeler AB**, Van Deusen AL, Gadani IC, Williams CM, Goggin SM, Hirt AK, Vradenburgh SA, Fread KI, Puleo EA, Jin L, *et al.* (2022) A developmental atlas of somatosensory diversification and maturation in the dorsal root ganglia by single-cell mass cytometry. *Nat. Neurosci* **25**:1543-1558 <https://doi.org/10.1038/s41593-022-01181-8> | [PubMed](#)

48. **Vradenburgh SA**, Van Deusen AL, Beachum AN, Moats JM, Hirt AK, Deppmann CD, Keeler AB, Zunder ER (2023) Sexual dimorphism in the dorsal root ganglia of neonatal mice identified by protein expression profiling with single-cell mass cytometry. *Mol. Cell. Neurosci* **126** <https://doi.org/10.1016/j.mcn.2023.103866> | PubMed
 49. **Kumar S**, Kahle AD, Keeler AB, Zunder ER, Deppmann CD (2025) Characterizing Microglial Signaling Dynamics During Inflammation Using Single-Cell Mass Cytometry. *Glia* **73**:1022-1035 <https://doi.org/10.1002/glia.24670> | PubMed
 50. **Shi J**, Liu W, Song A, Sanni T, Van Deusen A, Zunder ER, Deppmann CD (2025) Extrinsic apoptosis and necroptosis in telencephalic development: a single-cell mass cytometry study. *Cell Death Differ* <https://doi.org/10.1038/s41418-025-01594-5> | PubMed
 51. **Van Deusen AL**, Kumar S, Calhan OY, Goggin SM, Shi J, Williams CM, Keeler AB, Fread KI, Gadani IC, Deppmann CD, *et al.* (2025) A single-cell mass cytometry-based atlas of the developing mouse brain. *Nat. Neurosci* **28**:174-188 <https://doi.org/10.1038/s41593-024-01786-1> | PubMed
 52. **Fread KI**, Strickland WD, Nolan GP, Zunder ER (2017) An updated debarcoding tool for mass cytometry with cell type-specific and cell sample-specific stringency adjustment. *Pac Symp Biocomput* **22**:588-598 https://doi.org/10.1142/9789813207813_0054 | PubMed
 53. **Zunder ER**, Finck R, Behbehani GK, Amir E.-AD, Krishnaswamy S, Gonzalez VD, Lorang CG, Bjornson Z, Spitzer MH, Bodenmiller B, *et al.* (2015) Palladium-based mass tag cell barcoding with a doublet-filtering scheme and single-cell deconvolution algorithm. *Nat. Protoc* **10**:316-333 <https://doi.org/10.1038/nprot.2015.020> | PubMed
 54. **Behbehani GK**, Thom C, Zunder ER, Finck R, Gaudilliere B, Fragiadakis GK, Fantl WJ, Nolan GP (2014) Transient partial permeabilization with saponin enables cellular barcoding prior to surface marker staining. *Cytometry A* **85**:1011-1019 <https://doi.org/10.1002/cyto.a.22573> | PubMed
 55. **Finck R**, Simonds EF, Jager A, Krishnaswamy S, Sachs K, Fantl W, Pe'er D, Nolan GP, Bendall SC (2013) Normalization of mass cytometry data with bead standards. *Cytometry A* **83**:483-494 <https://doi.org/10.1002/cyto.a.22271> | PubMed
 56. **Schuyler RP**, Jackson C, Garcia-Perez JE, Baxter RM, Ogolla S, Rochford R, Ghosh D, Rudra P, Hsieh EWY (2019) Minimizing batch effects in mass cytometry data. *Front. Immunol* **10**:2367 <https://doi.org/10.3389/fimmu.2019.02367> | PubMed
 57. **Traag VA**, Waltman L, van Eck NJ (2019) From Louvain to Leiden: guaranteeing well-connected communities. *Sci. Rep* **9**:5233 <https://doi.org/10.1038/s41598-019-41695-z> | PubMed
 58. **Van Deusen AL**, Goggin SM, Williams CM, Keeler AB, Fread KI, Cheng I, Deppmann CD, Zunder ER (2022) A developmental atlas of the mouse brain by single-cell mass cytometry. *bioRxiv* <https://doi.org/10.1101/2022.07.27.501794>
 59. **McInnes L**, Healy J, Saul N, Großberger L (2018) UMAP: uniform manifold approximation and projection. *JOSS* **3** <https://doi.org/10.21105/joss.00861>
 60. **Becht E**, McInnes L, Healy J, Dutertre C.-A, Kwok IWH, Ng LG, Ginhoux F, Newell EW (2018) Dimensionality reduction for visualizing single-cell data using UMAP. *Nat. Biotechnol* **37**:38-44 <https://doi.org/10.1038/nbt.4314> | PubMed
- Sewell JM** (2025) 2025-05-13 BDNF_Rescue_FullSampleSet. Cytobank. ID 121988 <https://community.cytobank.org/cytobank/experiments/121988>

Peer reviews

Reviewer #1 (Public review):


The manuscript by the Deppmann group is an important contribution to understanding how growth factor signaling is controlled at a per-cell basis, in contrast to bulk biochemistry results. Their system uses cell culture and single-cell signalling proteomics methods to measure responses of cells of different developmental stages (from E14 rat) with complex but

relatively clear-cut phenotypes, allowing the effects of BDNF to be compared. This work validates the method for the discovery of future insights from less well-studied ligand-receptor investigations.

Strengths include:

- (1) The methods are cutting-edge and powerful.
- (2) Clearly written. It leads the reader through the rationale of methodological steps.
- (3) Step-by-step data interrogation rather than leaping into complex models of analysis.
- (4) "sanity check" controls e.g., mimicking bulk culture expected signaling /expression changes.
- (5) Testing biologically of certain findings within the presentation of the results (e.g., progenitors not responding to BDNF also not internalising TrkB).
- (6) Effort to make complex figures/data as understandable as possible.
- (7) Not overstating conclusions.
- (8) Important conclusion of receptor stoichiometry sets the potential for BDNF sensitivity, and that the intrinsic environment allows for a cell to engage that potential, something possibly thought but not demonstrated previously.

Major points:

- (1) Apply appropriate statistics: Student's t-tests are used throughout. It would be more appropriate to utilise ANOVA, at least one-way, to compare across timepoints for a given phospho-protein within one treatment condition (e.g., pERK following BDNF stim), or even multiple t-tests. Also, multiple testing adjustments. are likely needed (not my expertise).
- (2) Some data points are n=2; for statistical rigour n=>3 would be appropriate.
- (3) They measured pTrkB with antibody targeting site Y816, which couples to PLC γ /PKC/Ca $^{2+}$, but not Shc (for PI3K/MEK pathways), why? Did they get any measurements using an antibody targeting the phosphorylation sites in the activation loop of the kinase? Could this explain the relatively low abundance of active TrkB, compared to the measured TrkB-dependent signalling outcomes? Especially considering the "unresponsive" cells. E.g. [https://doi.org/10.1016/S0896-6273\(00\)00035-0](https://doi.org/10.1016/S0896-6273(00)00035-0) .
- (4) Was TrkC (or A) expressed in any TrkB population that could potentially mediate BDNF signaling?
<https://doi.org/10.7554/eLife.111513.1.sa2>

Reviewer #2 (Public review):

In this study, Sewell et al. use a novel approach to understand cell-specific BDNF signaling in the developing spinal cord. Using cultured E14 spinal cord, the authors used a mass cytometry approach to identify the levels of TrkB and p75NTR receptor expression, as well as 19 signaling markers and cell identification markers, to delineate activation of BDNF signaling in different cell types within a complex population. They identified that the level of receptor expression, while necessary, is not sufficient to determine the activation of signaling cascades. It has been known for some time that TrkB, indeed all RTKs, have the capacity to activate certain canonical signaling pathways; however, not all these pathways are always activated upon ligand treatment. This study begins to identify the conditions under which

specific signaling pathways are activated by ligand. Specifically, the type of cell and maturation state are critical for determining signaling. The cytometry approach allows the clustering of cell types according to expression of specific markers, and overlaying those clusters onto the expression status of TrkB and p75 receptors, as well as specific activated signaling proteins. This study provides greater insight into when specific signaling events can be activated by BDNF than was previously known.

The comparison of levels of expression of TrkB and p75NTR is interesting to demonstrate which pathways may require one or both receptors for specific signaling responses.

It is very interesting that progenitors do not respond to BDNF despite abundant expression of TrkB, although they responded to the rescue treatment with phosphorylation of Erk and Akt. The development of competence to respond to BDNF is an interesting question for future analysis, and the authors suggest some possibilities in their Discussion.

The responses of glial cells in their culture preparation are also interesting. They see signaling responses to BDNF in astrocytes and "laden" microglia (presumably phagocytic). E14 spinal would not be expected to have a large population of glia at this stage of development, although the serum in their plating media would allow for the proliferation of the progenitors. Astrocytes are generally considered to have the truncated TrkB receptor, yet they see P-Erk, P-Akt, etc. in these cells in response to BDNF. This raises the question of which receptors are expressed in the glial populations and whether the responses in these cells are also maturation dependent, since the glia in their culture conditions are also likely to be immature.

Some specific comments:

(1) The authors should specify what is meant by "rescue" in the text. What is rescuing the cells from trophic deprivation when no BDNF is added? Is it the B27 and GlutaMax in the Maintenance media, and does this actually rescue the cells?

(2) Figure 3 - K252a blocked activation in most, but not all, lineages, especially in mature neurons. Is some component of the P-Erk activation in these cells TrkB independent?

(3) Figure 5 E, F - The correlation between receptor surface depletion and signaling is based on "surface-specific staining". Does the staining allow you to see internalized receptors to confirm that the receptors are internalized?

(4) The drawbacks to the study - particularly capturing snapshots in time to represent signaling cascades, are fully acknowledged in the Discussion. The interplay between TrkB-T1, TrkB-FL, and p75NTR cannot be elucidated from this study, but again, that is acknowledged and will require a different approach.

<https://doi.org/10.7554/eLife.111513.1.sa1>

Reviewer #3 (Public review):

This study addresses a fundamental and long-standing question in neurotrophin biology, how cellular context shapes the interpretation of a single trophic message, and tackles it with a technically demanding and well-executed single-cell mass cytometry approach. By simultaneously measuring 19 signaling effectors and 18 identity markers across a developmental gradient of spinal cord cell types, the authors substantially expand our understanding of BDNF signaling and provide a compelling demonstration of the limitations inherent to bulk biochemical readouts, which average across heterogeneous populations and obscure the discrete subpopulation behavior that the present data reveal.

The finding that only 47-75% of cells respond at peak activation, that maturation state dictates both the magnitude and the qualitative "signature" of the response, and that identical receptor stoichiometries can yield divergent outcomes across cell types collectively constitute an important conceptual advance. The proposed framework of "prepared competence" is thought-provoking and likely to stimulate follow-up work.

That said, several aspects of the data interpretation deserve more critical discussion. My specific comments are detailed below.

(1) Interpretation of TrkB-independent ERK activation (lines 194-196).

The authors state that the residual pERK induction observed in TrkB-negative ("None") cells and the incomplete suppression of pERK by K252a support the established notion that BDNF signaling is not mediated solely through TrkB. This interpretation is presented without sufficient mechanistic detail and, in its current form, is difficult to follow. If BDNF-induced ERK activation is not mediated by TrkB, which alternative receptors could account for it? Does this reflect signaling through p75NTR, transactivation of other receptor tyrosine kinases, or another mechanism altogether? Likewise, the partial resistance of pERK to K252a is interpreted as evidence of an additional regulatory layer, but the underlying activity is not specified. Is the authors' hypothesis that a distinct pool of ERK is engaged independently of Trk activity? If so, what kinase activity is proposed to drive it? These results are intriguing yet puzzling and merit a more critical and explicit discussion of the candidate mechanisms.

(2) The "progenitor paradox" in light of prior work on PC12 cells (lines 207-208).

The observation that TrkB-expressing progenitors remain insensitive to BDNF is presented as a paradox and interpreted through the lens of impaired internalization. This interpretation would benefit from explicit discussion in the context of the classical work on PC12 cells (Segal and colleagues, among others), which established that plasma membrane-restricted Trk receptors engage the Ras-MAPK pathway with rapid, short-duration kinetics that drive proliferation rather than differentiation, whereas internalized Trk receptors sustain MAPK signaling and promote differentiation. Under this framework, the apparent signaling silence of progenitors could, in fact, reflect transient plasma membrane signaling that the time points sampled in the present study (5 min onward) may not capture. The single-cell mass cytometry approach used here is, in principle, well-suited to resolving such rapid kinetics, and the authors are encouraged to address this possibility, both as an alternative interpretation of their data and as a potential extension of the study.

(3) Astrocyte responsiveness and the TrkB isoform issue.

The authors report that astrocytes are highly responsive to BDNF and exhibit robust ligand-induced depletion of surface TrkB, which they interpret as evidence of signaling-competent full-length TrkB (TrkB-FL) on these cells. However, it is well established that astrocytes predominantly express the truncated isoform TrkB-T1, which lacks the intracellular kinase domain and is thought to function in BDNF capture, clearance, and recycling at synapses rather than in canonical downstream signaling. The robust phosphorylation events observed in astrocytes are therefore difficult to reconcile with TrkB-T1-mediated signaling alone. Could these responses instead reflect transactivation of other receptors through neuron-astrocyte crosstalk, for instance, via ligands released by neurons in response to BDNF? Because the authors explicitly state that their antibody cannot distinguish TrkB-FL from TrkB-T1, this limitation directly impacts the interpretation of the astrocyte data and of the proposed isoform-switch hypothesis for progenitors. This caveat is briefly acknowledged but deserves more thorough discussion, ideally with explicit consideration of the alternative interpretations outlined above.

(4) Pathways resistant to K252a inhibition.

The authors note that K252a fails to fully abolish pERK induction in several lineages, but the specific pathways, differentiation states, and receptor stoichiometries that remain K252a-resistant are currently insufficiently described. A more systematic description would strengthen this section. In addition, it would be helpful to discuss whether the residual signal could reflect the proximity of the response to the detection threshold rather than a genuinely K252a-insensitive pool of activity. More broadly, K252a is a broad-spectrum tyrosine kinase inhibitor with well-documented off-target effects, and the present study relies on this single pharmacological tool to define Trk-dependence. The limitations of this approach, and the desirability of complementary inhibitors or genetic perturbations in future studies, should be acknowledged in the Discussion.

(5) The 12-hour trophic deprivation paradigm as a potential confounder.

All cells in the present study are trophically deprived for 12 hours prior to stimulation. This is a methodologically convenient choice, but sustained deprivation is not a neutral starting point: it activates stress-responsive pathways (JNK, p38, autophagy), alters receptor surface trafficking, and can sensitize cells to subsequent stimulation. Several of the reported observations - including the apparent synergy of p75NTR with TrkB on stress markers (p-c-Jun, p38) and the strong induction of trophic effectors immediately upon BDNF addition - could be amplified, or qualitatively altered, by the prior deprivation state, which does not reflect baseline *in vivo* physiology. The Rescue control, with complete medium, partially addresses this concern but is non-specific. The authors should explicitly acknowledge this limitation and, ideally, discuss the extent to which their conclusions about cell-type-specific signaling competence depend on the deprivation paradigm.

(6) Direct comparison of pseudobulk data with conventional bulk biochemistry.

The pseudobulk reconstruction of the single-cell data is presented as recapitulating canonical BDNF responses, but this comparison relies on general agreement with the published literature rather than on a direct, parallel measurement in the same cultures. Given that the central conceptual contribution of the manuscript rests precisely on departures from the bulk biochemical view of BDNF signaling, an explicit side-by-side comparison of the pseudobulk profile against a parallel bulk Western blot from sister cultures - for at least a subset of key markers such as pERK, pAkt, and pCREB - would substantially strengthen the validation of the platform. Such a comparison would reassure the reader that the discrete subpopulation behavior reported here is genuinely biological, and not in part a consequence of methodological differences between mass cytometry and conventional biochemistry (e.g., differences in fixation kinetics, epitope accessibility, or sensitivity to low-abundance phosphoproteins).

(7) Manuscript organization and balance between main and supplementary figures.

The manuscript presents an exceptionally rich dataset, but the current organization - seven main figures supported by thirteen supplementary figures, several of which are explicitly labeled as extensions of main-text figures - makes it difficult to follow the argument without continuous cross-referencing between documents. I would encourage the authors to consider a substantive reorganization with the following suggestions: (i) Figure S2 and Figure S3, which respectively define the threshold-based "responsiveness" criterion and assess its robustness, are foundational to the central 47-75% responsiveness claim and would be better integrated into the main text, for example as additional panels of Figure 2; (ii) the methodological and quality-control components of Figure S1 and Figure S2 would be more naturally placed within the Methods section; and (iii) the four "Extension" figures (S4, S7, S12, S13) contain considerable redundancy with the corresponding main figures and could be consolidated, with only the most diagnostic panels retained. Concurrent trimming of the denser main figures (Fig. 4, 5, and 6 each carry six or seven panels) would further improve readability.

<https://doi.org/10.7554/eLife.111513.1.sa0>